Korean J. Chem. Eng., **27**(4), 1099-1108 (2010)
DOI: 10.1007/s11814-010-0172-0

4-Lump kinetic model for vacuum gas oil hydrocracker involving hydrogen consumption

Sepehr Sadighi*,†, Arshad Ahmad*, and Mehdi Rashidzadeh**

*Universiti Teknologi Malaysia, Faculty of Chemical and Natural Resources Engineering, 81310 UTM Skudai, Johor Bahru, Malaysia
**Catalysis Research Center, Research Institute of Petroleum Industry, P.O. Box 14665-137, Tehran, Iran
(*Received 9 September 2009 • accepted 4 November 2009*)

Abstract−A 4-lump kinetic model including hydrogen consumption for hydrocracking of vacuum gas oil in a pilot scale reactor is proposed. The advantage of this work over the previous ones is consideration of hydrogen consumption, imposed by converting vacuum gas oil to light products, which is implemented in the kinetic model by a quadratic expression as similar as response surface modeling. This approach considers vacuum gas oil (VGO) and unconverted oil as one lump whilst others are distillate, naphtha and gas. The pilot reactor bed is divided into hydrotreating and hydrocracking sections which are loaded with different types of catalysts. The aim of this paper is modeling the hydrocracking section, but the effect of hydrotreating is considered on the boundary condition of the hydrocracking part. The hydrocracking bed is considered as a plug flow reactor and it is modeled by the cellular network approach. Initially, a kinetic network with twelve coefficients and six paths is considered. But following evaluation using measured data and order of magnitude analysis, the three route passes and one activation energy coefficient are omitted; thus the number of coefficients is reduced to five. This approach improves the average absolute deviation of prediction from 7.2% to 5.92%. Furthermore, the model can predict the hydrogen consumption for hydrocracking with average absolute deviation about 8.59% in comparison to those calculated from experimental data.

Key words: Vacuum Gas Oil, Hydrotreating, Hydrocracking, Lump Kinetic Model, Hydrogen Consumption

INTRODUCTION

Crude oils contain a large fraction of heavy products for which only few outlets exist. Indeed, the world demand for light and middle distillate continually increases, while at the same time, the available crude oil becomes heavier [1]. Therefore, upgrading of heavy crude oil fractions to more useful lighter products is indispensable. Hydrocracking is one of the most important processes in a modern refinery to produce low sulfur diesel. The versatility and flexibility of the process makes it economically attractive to convert different types of feedstock into various yields including gas, LPG, naphtha, kerosene and diesel, leading to its widespread applications. Among all the commercially proven technologies for heavy fraction hydrocracking, those using fixed-bed reactors in series charged with different functionalities are very favorable. But, the main disadvantage of fixed-bed reactors is the loss of catalyst activity over time as a result of catalyst deactivation which reduces drastically the length of run [2]. In the particular case of vacuum gas oils (VGO), a previous HDT stage, first stage, for removing nitrogen, sulfur and metal compounds as well as saturation of polynuclear aromatics (PNA) to preserve catalyst from fast deactivation is required [3]. During the HDT process a portion of the hydrogen, dependent on HDS and HDN reactions, is consumed and most of the heavy sulfur and nitrogen compounds are converted to lighter products. Therefore, it can be concluded that a part of the desirable products and consumed hydrogen are the share of HDT in the first stage which should be considered during kinetic modeling of hydrocracking reactions in the second stage.

Typical of industrial processes, optimal operation is required to guarantee profitability, and such a task necessitates the use of process models. These models are used to predict the product yields and qualities, and are useful for sensitivity analysis, so that the effect of operating parameters such as reactor temperature, pressure, space velocity, as well as others on product yields and qualities can be understood. The models can also be used for process optimization and control, design of new units and selection of suitable hydrocracking catalysts [4]. However, the complexity of hydrocracking feed makes it extremely difficult to characterize and describe its kinetics at a molecular level [5]. One way of simplifying the problem is to consider the partition of the species into a few equivalent classes, the so-called lumps or lumping technique, and then assume each class is an independent entity [6]. This approach is attractive for kinetic modeling of complex mixtures because of its simplicity [7].

Mosby et al. [8] reported a model that describes the performance of a residue hydrotreater using lump first-order kinetics. The proposed model divides residue into lumps that are "easy" and "hard" crack. This lumping scheme was used by Aboul-Gheit [9] to determine the kinetic parameters of vacuum gas oil (VGO) hydrocracking, expressing composition in molar concentration. In his four-lump kinetic model, VGO was converted to gases, gasoline, and middle distillates. The model had eight kinetic constants that were estimated by experiments performed in a fixed-bed plug flow micro

†To whom correspondence should be addressed.
E-mail: sadighi_sepehr@yahoo.com

reactor. Ayasse et al. [10] fitted experimental product yields from catalytic hydrocracking of Athabasca bitumen obtained in a continuous-flow mixed reactor. In this model, the data were all obtained at a constant temperature, so the Arrhenius parameters of the rate constants were only valid in a narrow operating range. Moreover, the model was stoichiometric base and was significantly model-dependent. Therefore, the model was not recommended for more than five lumps. Cellejas and Martinez [11] studied the kinetics of Maya residue in a perfectly mixed reactor in continuous operation in the presence of a hydrotreating commercial catalyst. They used a first-order kinetic model with a 3-lump configuration which was atmospheric residue, lights oil and gases. The six kinetic constants in the model were estimated by experimental data. The model represented good validation at 375 and 400 °C, but at 415 °C the fits were bad. Another kinetic model for gas oil hydrocracking was proposed by Yui and Sandford [12]. In this case, pilot scaled experiments were performed in a trickle-bed reactor at various different operating conditions. Their model was also a 3-lump kinetic model, and similarly, the four kinetic constants were estimated from experimental data. Anchyeta et al. [13] proposed a 5-lump kinetic model for catalytic cracking of gas oil in which the deactivation of catalyst was considered as an exponential law with one decay parameter depending on the time-on stream. The model had eight kinetic constants, including one for catalyst deactivation which was estimated from experiments obtained in a microactivity reactor (MAT). Product yields predicted by this model showed a good agreement with experimental data with average deviation less than 2%. Aoyagi et al. [14] studied the kinetics of hydrotreating and hydrocracking of conventional gas oil, coker gas oils and gas oils derived from Athabasca bitumen. The model used a first-order expression and 3-lump kinetic network to describe the reaction of heavy gas oil. Their experiments were performed in fixed condition (constant temperature, pressure and LHSV) and the model predicted the results acceptably. Sanchez et al. [15] proposed a five-lump kinetic model with 10 kinetic parameters for moderate hydrocracking of heavy oils. These parameters were estimated from experimental data obtained in a fixed-bed down-flow reactor with Maya heavy crude. The lumps adopted for the study were residue, VGO, distillates, naphtha and gases. This kinetic model predicted well the hydrocracking process of Maya heavy oil at moderate pressure and temperatures in a down-flow experimental reactor.

Singh et al. [16] also adopted a 5-lump modeling strategy in predicting the yield of mild thermal cracking of vacuum residue. The lumping scheme chosen was based on the most value added products, i.e., gas, gasoline, light gas oil and vacuum gas oil. In this case, the model had seven kinetic parameters.

Almeida et al. [17] presented a 5-lump kinetic model for hydroconversion of Marlim vacuum residue in which by utilizing fourteen experiments in batch reactor, 26 coefficients were estimated for the kinetic model.

One of the recent works using the lumping method was the dynamic simulation of hydrotreating operation presented by Remesat et al. [18]. This work confirmed the validity of lumping strategy even for the hydrotreating process. The usage of lumping strategy is not limited to hydrocracking and some works have been done in the similar fields like modeling of fluid catalytic cracking process [19], hydroconversion [20] and catalytic [21,22] as well as thermal cracking [23] of heavy oils which the latter is in the field of petrochemical processes.

In the present study, a model for a dual bed pilot scale hydrocracking unit has been developed. The first section bed of the reactor is charged with hydrotreating catalyst to eliminate the amount of impurities in the VGO to produce low sulfur and nitrogen products and preserve the hydrocracking catalyst loaded in the second bed. The model presented in this paper only considers the hydrocracking part, but the effect of hydrotreating section has also been considered in the boundary conditions of the hydrocracking catalyst. Although there are only four lumps involved in this investigation, the main advantage of that over those previously reported in the literature is consideration of the hydrogen consumption in kinetic

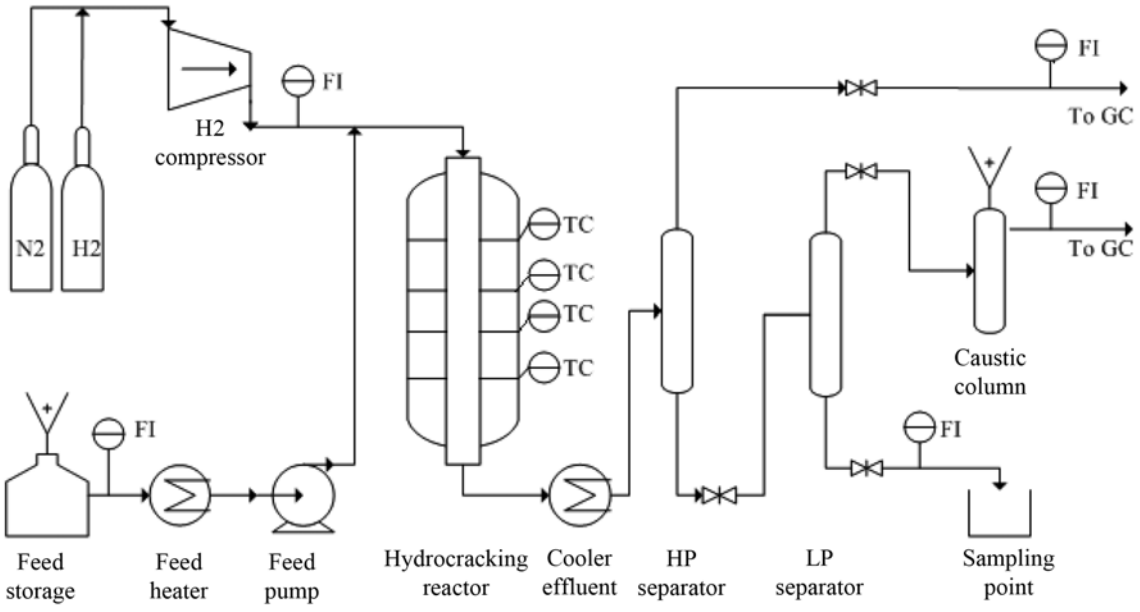

Fig. 1. Simplified process flow diagram of hydrocracking set up.

equations and overall mass balance. The present model according to 4-lump approach is simplistic, but as it can be concluded later, the model can predict the yield of hydrocracking products and hydrogen consumption reasonably adequately.

EXPERIMENTAL

1. Pilot Plant Device

Hydrotreating (HDT) and Hydrocracking (HDC) of VGO are performed in a high pressure test plant ('BASF') (Fig. 1). The reactor is designed as a tube with an inside diameter of 16 mm and total length of 2,160 mm which is subdivided into four sections. The first section, having a length of 100 mm, is packed with inert SiC particles. This entrance section is used to provide a uniform distribution of gas and liquid. The two following sections with a length of 355 mm and 865 mm are loaded with 63.5 cm^3 hydrotreating and 152 cm^3 hydrocracking catalysts, respectively. The final section is also contained with 50mm of inert. The SiC diameter lies in the 1.5-2.5 mm range.

In all experiments reported in this paper a single charge of both catalysts is used. The temperature along the reactor bed is controlled by use of four thermocouples. Therefore, an isothermal condition is maintained along the active reactor section.

2. Catalyst

In the present investigation two types of commercial hydrotreating and hydrocracking (zeolite-based) of VGO are used which are loaded in separate beds. The usage of zeolite based hydrocracking catalysts for upgrading of residue has been reported before [24]. The characteristics of HDT and HDC catalysts are presented in Table 1. Before loading, both catalysts are heated to 130 °C and are held at this temperature for about 6 hr for drying. Then, they are sulfided with an appropriate agent according to the manual of the catalyst vendor.

3. Feed and Product Characterization

The hydrocracking feed is prepared by blending of the fresh VGO and recycle feed (unconverted oil) taken from commercial Isomax unit which is located in Iran. The feed properties are shown in Table 3. Mixing ratio of fresh and recycle feed is 83.3 vol% and 16.7 vol%, respectively.

The main products of the process included gas (G), naphtha (N), distillate (D) and unconverted oil whilst its properties are assumed the same as VGO. According to Table 2, the latter assumption is not far from reality because of the negligible difference between distillation properties of these lumps. The average density and boiling point range of others are presented in Table 3. All properties of the feed and product samples are determined according to the ASTM standard procedures.

Table 1. Characteristics of HDT&HDC catalyst

Property	HDT	HDC
Size & Shape	1/16″& Quadralobe	1/16″& Cylindrical
Color	Green	Brown
Bulk density (kg/m^3)	750	850
BET surface area (m^2/g)	186.5	199.4
Langmuir surface area (m^2/g)	259.2	273.7
Average pore diam (A^0)	89.09	69.14
Main Ingredients	Mo, Ni, Ti	Zr, W, Ni, Si, Al

Table 2. Properties of fresh VGO and recycle feed

Property	Fresh VGO	Recycle feed
SP.GR@15.56 °C	0.8777	0.8738
Distillation range (vol%)		
ASTM D1160	°C	°C
IBP	329.7	287.8
10%	390.6	390.7
30%	423.2	430.1
50%	445.6	452.9
70%	475.1	478.3
90%	523.7	517.1
End point	567.1	561.3
Nitrogen (ppmwt)	800	200
Sulfur (wt%)	1.4	0.03
Asphalt & Resin (wt%)	<0.1	<0.1

Table 3. Average properties of hydrocracking product

Lump	Sp.gr@15 °C	IBP-FBP (°C)
Gas	0.35	40^-
Naphtha	0.75	40-160
Distillate	0.823	161-370

4. Test Conditions

Hydrocracking is performed under the following process conditions:

1. H_2/HC=1,357 Nm^3/Sm^3
2. LHSV=0.8, 0.9 and 1.05 hr^{-1}
3. Temperature=360 °C, 370 °C, 380 °C and 390 °C
4. Pressure=146 bar

The pressure and H_2/HC are selected as recommended by the catalyst vendor. The LHSV and start of run temperature in a commercial reactor are normally around 1 hr^{-1} and 380 °C; therefore, wider conditions for these variables are selected.

CHEMICAL REACTIONS

1. Hydrotreating Section

The following reactions are major reactions promoting in the hydrotreating of VGO [25]:

1-1. Hydrodesulfurization (HDS)

As a lumped sulfur compound in VGO, 4,6-dimethyl-dibenzothiophene is selected to take part in HDS reactions [26]. To remove sulfur from this compound, 2 molecules of hydrogen are required per sulfur atom to convert it to a hydrocarbon within the boiling range of diesel cut [27]. Therefore, by HDS reaction, the sulfur lump in VGO is converted to diesel and H_2S.

1-2. Hydrodenitrogenation (HDN)

Organonitrogen compounds in petroleum feedstock undergo hydrodenitrogenation to form ammonia and liquid hydrocarbon [28, 29]. Between alkyl amines, quinoline is one of the most relevant nitrogen compounds in VGO of which seven molecules of hydro-

gen per nitrogen atom are needed to convert it to a hydrocarbon liquid within the boiling range of naphtha cut [27].

1-3. Hydrodearomatization (HDA)

The aromatic compounds present in the feed oil are grouped into mono-, di-, tri- and polyaromatics [30]. It was reported that mono-aromatics are significantly more difficult to saturate [31] and the amount of tri- and poly aromatics in VGO is considerably lower than di-aromatics [32]. Therefore, saturation of di-aromatics is the most possible HDA reaction in VGO hydrotreating which needs two molecules of hydrogen [27].

2. Hydrocracking Section

In the hydrocracking part, catalyst converts complex ring compounds into light products by the following sequence of hydrocracking reactions [27]. All of them consume hydrogen which should be included in the product of the reactor to have an exact mass balance for the hydrocracking model.

MODELING APPROACH FOR HYDROCRACKING SECTION

This work considers the 4-lump mathematical model, i.e., VGO, distillate, naphtha and gas, to match main products in the pilot. The kerosene and diesel, also light and heavy naphtha are lumped together as distillate and naphtha cuts, respectively. Moreover, it is assumed that VGO (as hydrocracking feed) should consume hydrogen to be cracked to lighter cuts. Fig. 2 illustrates the process pathways associated with the mentioned strategy. Note that if all pathways of reactions are considered, the model would include twelve kinetic parameters which should be estimated using experimental data.

Mathematical models for a trickle-bed catalytic reactor can be complex due the many microscopic and macroscopic effects occurring inside the reactor: flow patterns of both phases, size and shape of a catalyst particles, wetting of the catalyst pores with liquid phase, pressure drop, intraparticle gradients, thermal effects and, of course, kinetics on the catalyst surface [30]. It is therefore more practical to reduce the complexity of the reactor, focusing only on momentous process variables. This suggests the development of simpler models that incorporates the fewest possible parameters. The following assumptions have been made in the development of the present model:

1. Hydrocracking is a first-order hydrocracking reaction. Since hydrogen is present in excess, the rate of hydrocracking can be taken to be independent of the hydrogen concentration [33].
2. A cell network pattern exists in the trickle bed reactor
3. The pilot reactor operates under isothermal conditions
4. Hydrogen feed is pure
5. The petroleum feed and the products are in the liquid phase in the reactor
6. The pilot unit is in steady state operation
7. Catalyst activity does not change with time; therefore simulation is only valid for start of run conditions.

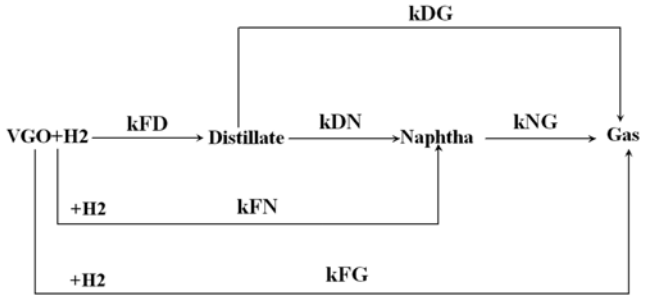

Fig. 2. The complete 4-lump kinetic model.

1. Axial Dispersion

To ensure that the reactor works at plug flow regime we have to survey whether backmixing can be neglected or not. A criterion reported by Mears [34] can be used to estimate the required minimum bed length L_b, so that backmixing effects can be ignored:

$$\frac{L_b}{d_p} > \frac{20n}{Pe_z} \cdot \ln\frac{1}{1-x} \tag{1}$$

In Eq. (1), L_b, catalyst bed length; d_p, particle diameter; n, order of reaction; x, fractional conversion; Pe_z, Peclet number, can be estimated as a function of Reynolds number. Depending on the correlation used for determining Pe_z, published by Froment and Bischoff [35] or Baerns et al. [36], the minimum ratio of L_b/d_p varies between 450 and 3,850, whereas the experimental ratio is 400.

For the current case, the particle diameter and the bed length are 0.211 mm and 122 cm, respectively. Consequently, L_b/d_p is about 578 for understudy reactor, enough higher than the minimum value. Hence, assuming the reactor as a plug reactor can be an acceptable assumption.

2. Kinetic Expression

For each reaction, a kinetic expression (R) is formulated as the function of mass concentration and kinetic parameters (k_0, E). Based on these assumptions, the kinetic constants of the proposed model are as in the following:

$$\text{Vacuum gas oil or Feed (F): } k_{Fj} = k_{0Fj}\exp\left(\frac{-E_{Fj}}{RT}\right) \tag{2}$$

Note thatin Eq. (2) represents diesel (D), naphtha (N) and gas (G)

$$\text{Diesel (D): } k_{Dj'} = k_{0Dj'}\exp\left(\frac{-E_{Dj'}}{RT}\right) \tag{3}$$

j′ in Eq. (3) represents naphtha (N) and gas (G).

$$\text{Naphtha (N): } k_{NG} = k_{0NG}\exp\left(\frac{-E_{NG}}{RT}\right) \tag{4}$$

In Eqs. (2) to (4), T and R are the bed temperature and ideal gas constant, respectively.

The reaction rates (R) can be formulated as the following:

$$\text{Vacuum gas oil reaction } (R_F): R_F = \sum_{j=D}^{G} k_{Fj} C_F \tag{5}$$

C_F in Eq. (5) is the mass concentration of VGO.

As depicted in Fig. 2, it is assumed for converting of VGO to hydrocracking products, hydrogen is added to the related path. Therefore, the net reaction rate for them can be described as the following:

$$\text{Diesel } (R_D): R_D = k_{FD} C_F (1+\alpha) - \sum_{j'=N}^{G} k_{Dj'} C_D \tag{6}$$

$$\text{Naphtha } (R_N): R_N = k_{FN} C_F (1+\alpha) + k_{DN} C_D - k_{NG} C_{NG} \tag{7}$$

$$\text{Gas } (R_G): R_G = k_{FG} C_F (1+\alpha) + k_{DG} C_D + k_{NG} C_N \tag{8}$$

In Eqs. (6) to (8), α shows the consumed unit mass of hydrogen per unit mass of converted VGO which is added to the molecular structure of products (diesel, naphtha and gas) during hydrocracking reactions. This coefficient is modeled by a quadratic polynomial equation [37] to predict the consumed hydrogen during the hydrocracking process as a response function of temperature (T) and LHSV as the following:

$$\alpha=\beta_0+\beta_1 T+\beta_2.LHSV+\beta_{11}.T^2+\beta_{22}.LHSV^2+\beta_{12}.T.LHSV \quad (9)$$

In this equation, β_0 is the intercept coefficient, β_1 and β_2 are the linear terms, β_{11} and β_{22} are the squared terms and β_{12} is the interaction term. These coefficients are estimated from experimental data and the adequacy of regression is checked with analysis of variance (ANOVA) using R-squared and Fischer F-test [37,38].

3. Mass Balance

Plug flow for fixed-bed reactors is assumed in many reported pilot scale reactor models that consist of a set of ordinary differential equation (ODEs) with defined boundary conditions. In this paper, to model the hydrocracking section, we implemented a cell network approach, the accuracy of which was confirmed for trickle bed reactors [39]. As shown in Fig. 3, the hydrocracking catalytic bed from the inlet to the outlet is divided into a number (N=200) of well-mixed cells that are grouped along the longitude direction. Mixing only occurs within each cell and backmixing is not accounted for between the adjacent cells. It is obvious that this approach is equivalent to a one-parameter non-ideal reactor model [40] that was adopted in some of the previous works in reactor modeling [41-43] in which by increasing the series reactor we can simulate the plug flow behavior.

In the interest of improving accuracy of the developed model, the volumetric flow rate in the reactor (ν) is considered variable and it is calculated according to the density of output stream of each cell (Eq. (11)). Finally, Eqs. (10) to (13) for each cell should be solved simultaneously to calculate the hydrocracking products.

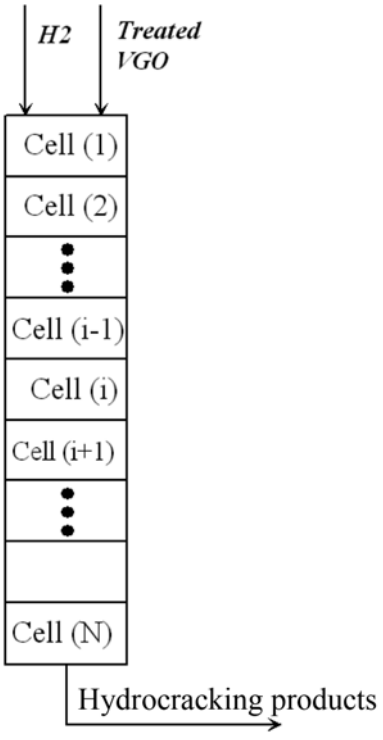

Fig. 3. Schematic representation of series mixed cells.

$$C_j(i-1)\nu(i-1)\pm\eta.\varepsilon.R_j(i)\times Vcat(i)=C_j(i)\nu(i) \quad (10)$$

$$\nu(i)=\frac{F_m(i)}{\rho(i)} \quad (11)$$

$$F_m(i)=\sum_{j=F}^{G} C_j(i)\,\nu(i) \quad (12)$$

$$Vcat(i)=\frac{V_b}{N} \quad (13)$$

In the above equations, the "–" is for reactant (feed or VGO), and the "+" sign is for the products; j, lumps from feed (F) to gas (G); C, the mass concentration of lumps; η, effectiveness factor; ε, bed void fraction; $F_m(i)$, mass flowrate in each cell; $V_{cat}(i)$ is the volume of hydrocracking catalyst in each cell; V_b is the volume of hydrocracking catalyst and N is the number of cells. The effectiveness factor for spherical catalyst in trickle bed regime and the bed void fraction is 0.7 [44] and 0.35, respectively.

The only unknown variable in the above equations is density of feed and product stream inside the reactor which can be calculated as follows:

$$\rho_0(i)=\sum_{j=F}^{G} Y_j(i)\rho_j \quad (14)$$

In Eq. (14), j is from feed (F) to gas (G), ρ_j is density of lumps. It should be noted that the density evaluated by this equation is standard density, which can be determined at reactor condition by the Standing-Katz correlation [45]. In deviating from the SI system we give the equation with the original units:

$$\rho_j(p, T)=\rho_0(i)+\Delta\rho_p(i)-\Delta\rho_T(i) \quad (15)$$

Where $\rho_0(i)$ represents the density at standard conditions in lb/ft^3. The pressure dependence can be evaluated by:

$$\Delta\rho_p(i)=[0.167+16.181\times10^{-0.0425.\rho_0(i)}].\left[\frac{p}{1000}\right] - 0.01\times[0.299+263\times10^{-0.0603.\rho_0(i)}].\left[\frac{p}{1000}\right]^2 \quad (16)$$

Where p is the pressure in psia. Since the density drops with ascending temperature, a temperature correction with the temperature T in ^{0}R is needed:

$$\Delta\rho_T(i)=[0.0133+152.4\times(\rho_0(i)+\Delta\rho_p(i))^{-2.45}].[T-520] - [8.1\times10^{-6}-0.0622\times10^{-0.764.(\rho_0(i)+\Delta\rho_p(i))}].[T-520]^2 \quad (17)$$

For parameter estimation, the sum of squared error, SQE, as given below, is minimized:

$$SQE=\sum_{k=1}^{N_t}\sum_{j=F}^{G}(Y_{jk}^{meas}-Y_{jk}^{pred})^2 \quad (18)$$

In Eq. (18), N_t, Y_{jk}^{meas} and Y_{jk}^{pred} are the number of test runs, measured product yield and the predicted by model, respectively.

The hydrocracking reaction model according to Eqs. (2) to (17) is coded and solved simultaneously by using Aspen Custom Modeler (ACM) programming environment (AspenTech, 2001) to evaluate the product yields (Y_i). Then Eq. (18) is minimized by sequencing

NL2Sol and Nelder-mead algorithm which are both in the Aspen Custom Modeler software. NL2Sol algorithm is a variation on Newton's method in which part of the Hessian matrix is computed exactly and part is approximated by a secant (quasi-Newton) updating method. To promote convergence from a poor initial point, a trust-region is used along with a choice of model Hessian. Hence, the approximate region is found with NL2Sol; then to fine tune the parameters, Nelder-Mead simplex method is used.

To evaluate the estimated kinetic parameters, average absolute deviation of predictions (AAD%) [46] is calculated by using the following expression.

$$AAD\% = 100 \frac{\sum_{k=1}^{N_t} \sqrt{\frac{(Y_k^{meas} - Y_k^{pred})^2}{Y_k^{meas^2}}}}{N_t} \% \quad (19)$$

RESULTS AND DISCUSSIONS

The effect of temperature on the yields of gas, naphtha, distillate and unconverted VGO (hydrocracking products) at three constant LHSVs (0.8, 0.9 and 1.05 hr^{-1}) was studied. We found that there are no abnormalities in the hydrocracking behavior of the catalyst in the experienced range. As expected, for gas, naphtha and distillate the temperature promotes the hydrocracking paths so that the yields of these products are increased. For the unconverted VGO or residue, temperature acts reversely so that it decreases the yield of residue. The effect of LHSV is in agreement with the rule of the smaller LHSV, the better the hydrocracking. Thus, converting of feed to gas, naphtha and diesel is always better in low LHSV. For the unconverted VGO or residue this reason acts reversely.

For all experiments (12 tests) it is found that the sulfur and nitrogen content of the hydrocracking product (mixture of naphtha, distillate and unconverted oil) are less than 100 and 50 ppmwt, respectively. Therefore, it is concluded that the hydrotreating catalyst can provide diesel with the sulfur content lower than 50 ppmwt which is desirable for a transport fuel.

The aromatic content of hydrocracking product in different LHSVs versus temperature is depicted in Fig. 4. As it can be concluded from this figure, the total aromatic content of the liquid products is reduced by temperature. But, LHSV has the reverse effect on that.

The mass flow rate of hydrogen consumption for each experiment is calculated by performing a mass balance around the system. We expect that the hydrogen consumption has been increased noticeably with raising the temperature and LHSV. But, as it was revealed from Fig. 5, our expectation is only satisfied for the temperature. It means the hydrogen consumption in constant LHSV

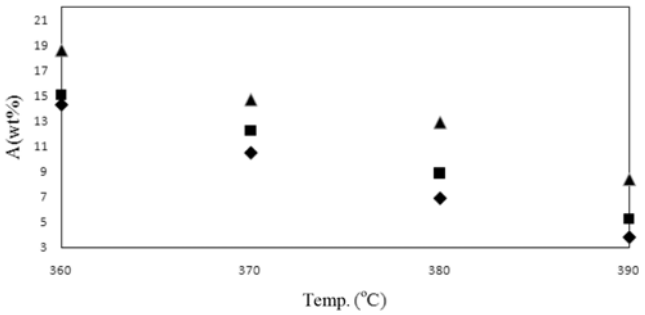

Fig. 4. Aromatic content vs. temperature. H_2/oil=1,357 Nm^3/Sm^3, pressure=146 bar (◆) LHSV=0.8 hr^{-1}, (■) LHSV=0.9 hr^{-1}, (▲) LHSV=1.05 hr^{-1}.

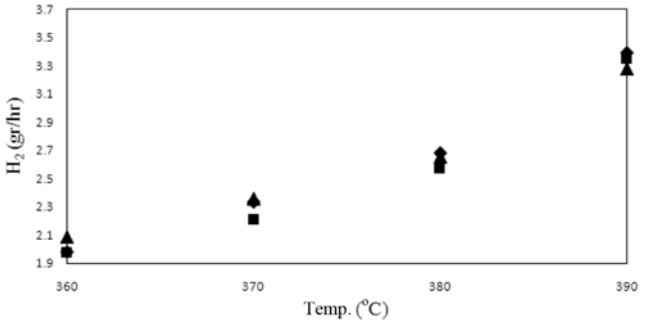

Fig. 5. Hydrogen consumption vs. temperature. H_2/oil=1,357 Nm^3/Sm^3, pressure=146 bar (◆) LHSV=0.8 hr^{-1}, (■) LHSV=0.9 hr^{-1}, (▲) LHSV=1.05 hr^{-1}.

increased sharply with temperature, but LHSV does not have any sensible variation on it. Even, in temperatures 380 °C and 390 °C, the hydrogen consumption is a little higher at lower LHSVs, discussed later.

Table 4 shows the yield of hydrocracking products, conventionally calculated on the basis of VGO input feed. The gas in this table is only composed of C_1, C_2, C_3, C_4 and a little amount of C_5, representing only hydrocracking products. As it can be seen, in most of the experiments we have more than 1% error in mass balance, mainly resulting from hydrotreating (HDS, HDN and HDA) reactions which are mainly performed in the hydrotreating section Therefore, the effect of hydrotreating reactions is on the boundary of the hydrocracking section, second catalytic bed, which can be considered according to the reactions mentioned in section 2.4.1.

To do this, at first hydrogen consumption is categorized to four main groups involved of HDS, HDN, HDA and HDC. According

Table 4. Yield percent of hydrocracking process based on the fresh VGO feed

T (°C)	360	370	380	390	360	370	380	390	360	370	380	390
LHSV(hr^{-1})	0.8	0.8	0.8	0.8	0.9	0.9	0.9	0.9	1.05	1.05	1.05	1.05
Gas%	1.71	2.54	2.81	3.23	1.37	1.66	2.23	2.86	1.17	1.30	1.64	1.99
Naphtha%	7.13	8.92	11.96	13.93	5.96	7.91	9.56	12.17	5.58	6.82	8.23	10.28
Diesel%	22.33	24.41	26.77	31.55	19.84	20.91	22.96	27.65	18.66	19.93	21.39	24.56
Residue%	67.53	63.12	57.67	50.94	71.47	68.33	64.22	56.55	73.24	70.63	67.56	62.08
Total	98.71	98.99	99.21	99.66	98.63	98.82	98.96	99.23	98.65	98.68	98.82	98.91

Table 5. Hydrogen consumption categorized to main reaction groups

T (°C)	360	370	380	390	360	370	380	390	360	370	380	390
LHSV(hr^{-1})	0.8	0.8	0.8	0.8	0.9	0.9	0.9	0.9	1.05	1.05	1.05	1.05
HDS (gr/hr)	0.37	0.37	0.37	0.37	0.42	0.42	0.42	0.42	0.49	0.49	0.49	0.49
HDN (gr/hr)	0.62	0.62	0.62	0.62	0.70	0.70	0.70	0.70	0.81	0.81	0.81	0.81
HDA (gr/hr)	0.23	0.28	0.33	0.37	0.24	0.29	0.34	0.39	0.22	0.29	0.32	0.40
HDC (gr/hr)	0.76	1.06	1.36	2.03	0.62	0.81	1.12	1.84	0.57	0.77	1.03	1.57
Total	1.980	2.335	2.681	3.392	1.977	2.209	2.575	3.349	2.089	2.360	2.656	3.280

Table 6. Product rates of the hydrotreating process

T (°C)	360	370	380	390	360	370	380	390	360	370	380	390
LHSV(hr^{-1})	0.8	0.8	0.8	0.8	0.9	0.9	0.9	0.9	1.05	1.05	1.05	1.05
Gas (gr/hr)	0	0	0	0	0	0	0	0	0	0	0	0
Naph. (gr/hr)	5.65	5.65	5.65	5.65	6.35	6.35	6.35	6.35	7.41	7.41	7.41	7.41
Dis. (gr/hr)	16.95	16.95	16.94	16.94	19.07	19.07	19.06	19.06	22.27	22.26	22.25	22.25
Res. (gr/hr)	131.51	131.56	131.61	131.65	147.94	147.98	148.03	148.09	172.61	172.68	172.72	172.80

to the assumptions presented in section 2.4.1, the required hydrogen for reduction of sulfur and nitrogen as well as aromatization is shown in Table 5.

The consumed hydrogen for hydrocracking is calculated by subtracting the hydrogen consumption for hydrotreating from total consumed hydrogen. Table 5 revealed this phenomenon that in a constant LHSV, the hydrogen consumption for hydrocracking is increased by temperature, but in constant temperature it is decreased by LHSV. Therefore, we suppose that a hydrocracking reaction is reversely affected by LHSV and it can be the reason for nuance variation of total hydrogen consumption by LHSV as shown in Fig. 5.

As it was discussed in the chemical reactions section, hydrotreating has a share in producing naphtha and diesel after converting sulfur and nitrogen compounds to H_2S and NH_3, respectively. For each corresponding reaction, a specific amount of hydrogen is consumed and H_2S, NH_3, naphtha and diesel products are determined by the amount of sulfur and nitrogen value in the VGO feed. Therefore, the feed emitted from hydrotreating, entered into the hydrocracking bed is composed of naphtha, diesel and purified VGO which are presented in Table 6. The produced naphtha and diesel should be subtracted from the final products to determine the performance of hydrocracking catalyst.

In Table 6, the production of gas in the hydrotreating section has been neglected, which can be a source of error, especially at high temperatures which is discussed later.

Up to now, the hydrogen consumption caused by hydrotreating reactions is considered in mass balances and the deflection resulting from them is healed. But, as it was mentioned before, a part of the hydrogen will be entered in the molecular structure of products during the hydrocracking reaction. To model this effect, considered by (α) in hydrocracking mathematical expression, the hydrogen consumed per converted VGO should be evaluated from experiments.

Fig. 6 shows the variation of hydrogen consumed (mgr) per converted VGO (gr) during hydrocracking reactions, representing by α, in the second catalyst bed. As discussed before, this value is increased directly by temperature, but LHSV has a reverse effect on that.

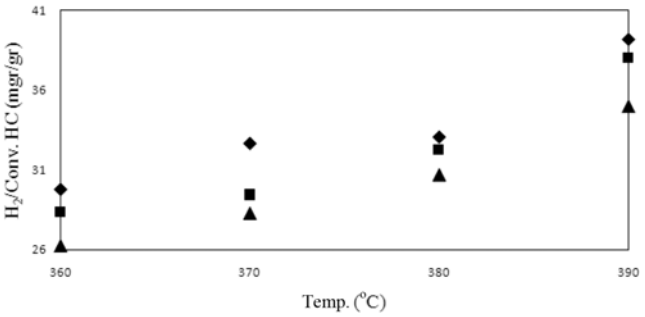

Fig. 6. Hydrogen consumption per converted hydrocarbon vs. temperature H_2/oil=1,357 Nm^3/Sm^3, pressure=146 bar (◆) LHSV=0.8 hr^{-1}, (■) LHSV=0.9 hr^{-1}, (▲) LHSV=1.05 hr^{-1}.

Table 7. Coefficient values for the responses α in Eq. (9)

Variable	β_0	β_1	β_2	β_{11}	β_{22}	β_{12}
T.LHSV	3441.319	−10.762	−18.906	0.00854	5.452	−0.00858

The α value is fitted to Eq. (9) using the regression analysis tool of Excel software (Microsoft office version 2007). The calculated coefficients are shown in Table 7. After that an ANOVA test is performed to evaluate the validity of the model. It confirmed that the quadratic model can predict α with an R^2 (R square) of about 0.9735 which is acceptable. Moreover, the adequacy of the fitted model is tested using static Fischer (F) with 1% critical level. The value of F=43.40 is higher than F(5, 6, 0.01)=8.47, demonstrating that the regressed model fitted well the observed values. The parity plot for measured and predicted by the quadratic model is presented in Fig. 7.

After achieving a model to predict α, twelve kinetic parameters needed for the 4-lump kinetic network (Fig. 1) are estimated by using measured pilot data. Table 8 shows the estimated values of apparent activation energies and frequency factors. In this table, the rate constants for all reactions are evaluated in the average operat-

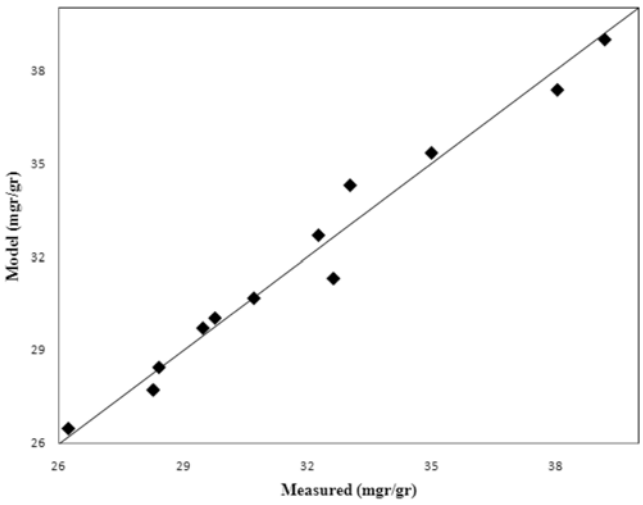

Fig. 7. Parity plots for quadratic model of hydrogen consumption for hydrocracking H_2/oil=1,357 Nm^3/Sm^3, pressure=146 bar (◆) LHSV=0.8 hr^{-1}, (■) LHSV=0.9 hr^{-1}, (▲) LHSV=1.05 hr^{-1}.

Table 8. Kinetic parameters for the complete network

Frequency factor ($m^3 \cdot hr^{-1} \cdot m^3\ cat^{-1}$)		Activation energy (kJ/mol)		Rate order	
k_{0FD}	6.64E+07	E_{FD}	23.01	k_{FD}	0.55
k_{0FN}	1.04E+08	E_{FN}	24.27	k_{FN}	0.33
k_{0FG}	0	E_{FG}	12.96	k_{FG}	0
k_{0DG}	0	E_{DN}	0.26	K_{DN}	0
k_{0DN}	5.10E+03	E_{DG}	23.75	k_{DG}	2.4E-5
k_{0NG}	2.7	E_{NG}	1.1E-6	K_{NG}	1

Table 9. The for the different strategies in the plug flow reactor

Lump	Complete network	Reduced network
Gas	12.41	9.32
Naphtha	8.81	7.17
Distillate	4.52	4.31
Un.VGO	3.05	2.88
Ave.	7.2	5.92

ing temperature (375 ºC). To compare the simulated and measured product values, average absolute deviation is calculated and presented in Table 9 with the name of the complete network. As it is found from this table, the for prediction of all yields by the resulting kinetic factors in Table 9 is about 7.2%, which we think it is acceptable in the wide range of testing conditions. The main source of error is outstanding deviation for prediction of gas, which will be discussed later.

Data in Table 8 reveal that rate constants for the conversion of feed to distillate (k_{FD}) and naphtha (k_{FN}) are not far from each other. This phenomenon is consistent with the literature [47,48] that reported zeolite hydrocracking catalysts have tendency to produce naphtha, not more than distillate, but higher than amorphous catalysts.

Moreover, it can be concluded that the lower tendency of the catalyst to convert distillate to naphtha as well as distillate to gas can

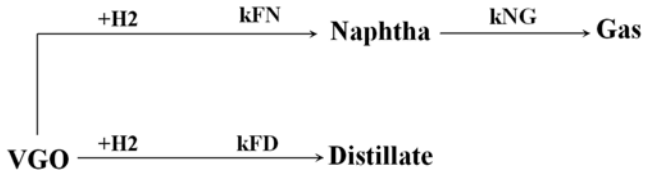

Fig. 8. The reduced 4-lump kinetic model.

Table 10. Kinetic parameters for the reduced network

Frequency factor ($m^3 \cdot hr^{-1} \cdot m^3\ cat^{-1}$)		Activation energy (kJ/mol)		Rate order	
k_{0FD}	4.26E+07	E_{FD}	22.43	k_{FD}	0.83
k_{0FN}	1.44E+10	E_{FN}	30.66	k_{FN}	0.54
k_{0FG}	0	E_{FG}	0	k_{FG}	0
k_{0DG}	0	E_{DN}	0	k_{DN}	0
k_{0DN}	0	E_{DG}	0	k_{DG}	0
k_{0NG}	2.06	E_{NG}	0	k_{NG}	1

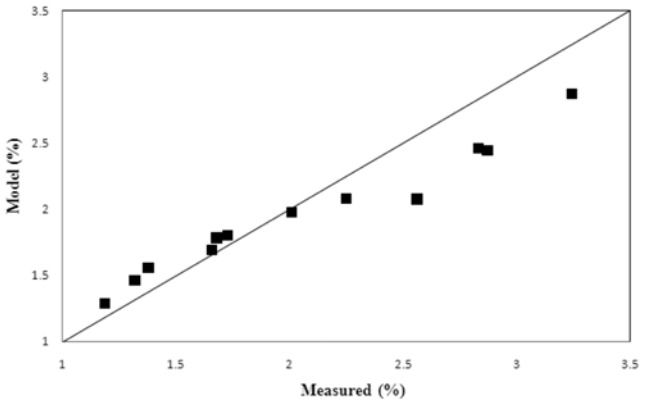

Fig. 9. Parity plot for gas resulted by reduced kinetic network H_2/oil=1,357 Nm^3/Sm^3, pressure=146 bar.

justify the higher yield of distillate in hydrocracking process. Also, we suppose that the high value for the rate of naphtha to gas is because of the simplicity of the cracking of naphtha's light chains in comparison to heavy chains of distillate and VGO, which seems a reasonable phenomenon.

Therefore, three paths which are VGO to gas, distillate to gas and distillate to naphtha can be ignored. Moreover, the activation energy of naphtha to gas is very low so that it can be omitted too. Finally, a reduced kinetic network results, depicted in Fig. 8. At this time, there are only five remaining kinetic constants which should be estimated. But, for that, there are forty-eight observations, making acceptable degree of freedom for parameter estimation procedure.

The reduced model is then estimated again using measured data, producing new coefficients as presented in Table 10. Upon comparing the measured data against the model predictions, the average AAD% for the reduced model is 5.92% which is dramatically improved in comparison to the complete network. This confirms the same situation for the claim of the previous work for thermal cracking that stated predictions using the reduced parameter model were more accurate [49].

The AAD% of all lumps resulted by reduced kinetic network is

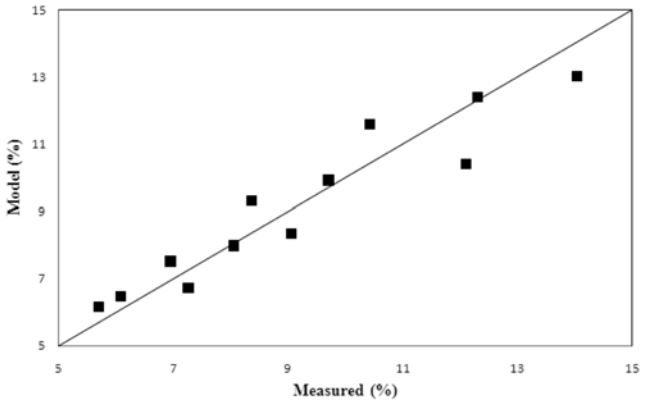

Fig. 10. Parity plot for naphtha resulted by reduced kinetic network H_2/oil=1,357 Nm^3/Sm^3, pressure=146 bar.

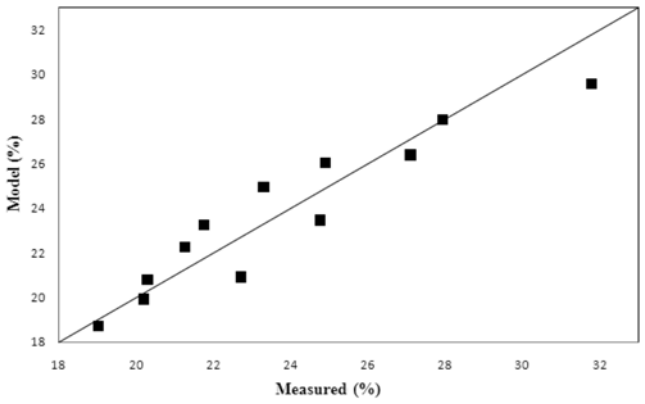

Fig. 11. Parity plot for distillate resulted by reduced kinetic network H_2/oil=1,357 Nm^3/Sm^3, pressure=146 bar.

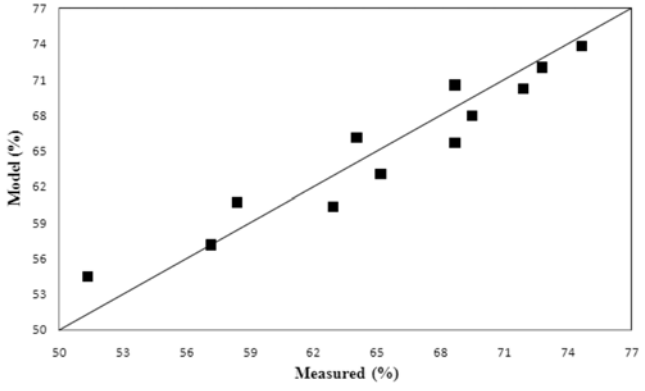

Fig. 12. Parity plot for residue resulted by reduced kinetic network H_2/oil=1,357 Nm^3/Sm^3, pressure=146 bar.

presented in Table 9 with the title of the reduced network.

The parity plots for measured data and model predictions are presented in Figs. 9 to 12, certifying the acceptable agreement between experimental and predicted values by the developed model. It is evident from these figures that the yield prediction of the reduced kinetic network is acceptable.

Furthermore it can be understood from Fig. 9 that the measured values for the yield of gas, related to high temperatures, are higher

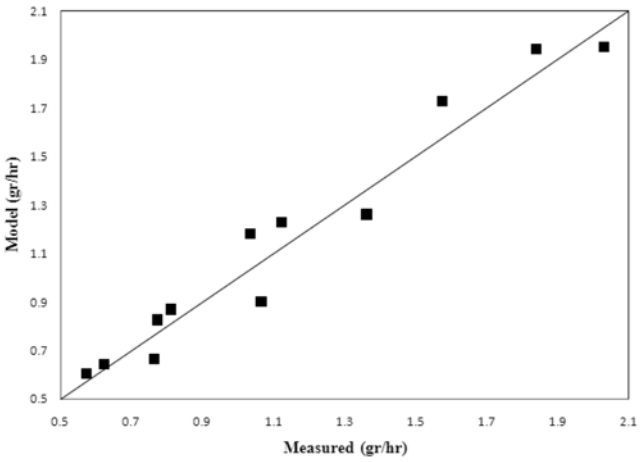

Fig. 13. Parity plot for hydrogen consumption of hydrocracking resulting from reduced kinetic network, H_2/oil=1,357 Nm^3/Sm^3, Pressure=146 bar.

than predicted by the model. We think that during the hydrotreating of VGO in the first catalytic section, there is the possibility for hydrocracking of light chains to gas, which is not included in the model, and the concentration of gas in the boundary of hydrocracking bed is assumed zero. Therefore, at high temperatures, fortifying this possibility, we have more deviation for gas prediction, which increases the AAD% of the model. The same reason can be interpreted for naphtha that some hydrocracking reactions can consume or produce naphtha in the hydrotreating section, not included in the model and they create more AAD% for this lump in comparison to diesel and VGO. We found that the mass balance error of the model for all predictions is less than 0.05%, confirming the exactness of the discussed approaches to decrease the error created by reducing impurities and adding hydrogen consumption. We think that the nuance error may be caused by nickel, vanadium or coke formation which was not included in the model.

Finally, the parity plot for hydrogen consumption in the hydrocracking section can be observed in Fig. 13. The AAD% for that is about 8.59%. We think that this error is natural because of the dependency of hydrogen consumption to yield of VGO, the latter of which has 2.88% error. Also, the quadratic model applied for calculation of needed hydrogen to VGO conversion has intrinsically a little deviation which is transferred to the kinetic model predictions.

CONCLUSIONS

In this research, a 4-lump kinetic model for gas oil hydrocracking was developed to predict the yield of gas, naphtha, distillate and hydrogen consumption of VGO hydrocracking in a pilot scale reactor charged with zeolite-base catalyst. Experiments were carried out in temperatures from 360 °C to 390 °C, LHSV from 0.9 to 1.05, H_2 pressure at 146 bar and H_2/oil at 1,357 Nm^3/m^3. The active zone of the reactor was divided into hydrotreating and hydrocracking sections, of which the effect of hydrotreating was considered according to HDS, HDN and HDA reactions reported in the literature. The hydrogen consumption of the hydrocracking reactions was implemented in the kinetic model of hydrocracking by use of a quadratic

response surface model which modeled the unit mass of hydrogen consumed per unit mass of converted VGO. The data generated in the pilot plant reactor were used to estimate kinetic parameters for each involved hydrocracking reaction and coefficients of hydrogen consumption model. The results showed that the reduced kinetic network could predict the experimental data with average deviation about 5.92%, which was 1.28% more accurate than the complete network. Moreover, the hydrogen consumption for hydrocracking of VGO to light products was predicted with 8.59% average absolute deviation.

The advantage of this model over the previous ones is implementing of hydrogen in the mass balance equation. This is important not only to have a less error yield prediction, but also to evaluate the hydrogen consumption of hydrocracking catalyst which is momentous as an economical variable.

REFERENCES

1. J. J. Vestraete, K. Le Lannic and I. Guibard, *Chem. Eng. Sci*., **62**, 5402 (2007).
2. A. Alvarez and J. Ancheyta, *Appl. Catal. A: Gen.*, **351**, 148 (2008).
3. A. Alvarez and J. Ancheyta, *Chem. Eng. Sci*., **63**, 662 (2008).
4. G. Valavarasu, M. Bhaskar and B. Sairam, *Petrol. Sci. Technol.*, **23**, 1323 (2005).
5. J. Ancheyta-Juarez, F. Lopez-Isunza and E. Aguilar-Rodriguez, *Appl. Catal. A: Gen.*, **177**, 227 (1999).
6. F. J. Krambeck, *Kinetics and thermodynamics lumping of multicomponent mixtures*, Elsevier, Amsterdam, 111 (1991).
7. J. Ancheyta, S. Sanchez and M. A. Rodriguez, *Catal. Today*, **109**, 76 (2005).
8. F. Mosby, R. D. Buttke, J. A. Cox and C. Nikolaids, *Chem. Eng. Sci*., **41**, 989 (1986).
9. K. Aboul-Gheit, *Erdol Erdgas Kohle*, **105**, 1278 (1989).
10. R. Ayasse, H. Nagaishi and E. W. Chan, *Fuel*, **76**, 1025 (1997).
11. M. A. Callejas and M. T. Martinez, *Ind. Eng. Chem. Res*., **38**, 98 (1999).
12. S. M. Yui and E. C. Sanford, *Ind. Chem. Res*., **28**, 319 (1989).
13. J. Ancheyta, F. Lopez and E. Aguilar, *Appl. Catal. A: Gen.*, **177**, 227 (1999).
14. K. Aoyagi, W. C. McCaffrey and M. R. Gray, *Petrol. Sci. Technol*., **21**, 997 (2003).
15. S. Sanchez, M. A. Rodriguez and J. Ancheyta, *Ind. Eng. Chem. Res*., **44**, 9409 (2005).
16. J. Singh, M. M. Kumar, A. K. Saxena and S. Kumar, *Chem. Eng. J*., **108,** 239 (2005).
17. R. M. Almeida and R. Guirardello, *Catal. Today*, **109**, 104 (2005).
18. D. Remesat, B. Young and W. Y. Surcek, *Chem. Eng. Res. Design*. In press.
19. F. van landeghem, D. Nevicato, I. Pitault, M. Forissier, P. Turlier, C. Derouin and J. R. Bernard, *Appl. Catal., A*, **138**, 381 (1996).
20. R. M. Almeida and R. Guirardello, *Catal. Today*, **109**, 104 (2005).
21. X. Meng, Ch. Xu, J. Gao and L. Li, *Appl. Catal. A: Gen.*, **301**, 32 (2006).
22. X. Meng, Ch. Xu, J. Gao and L. Li, *Catal. Communications*, **8**, 1197 (2007).
23. S. Zahedi, J. Towfighi, R. Karimzadeh and M. R. Omidkhah, *Korean J. Chem. Eng*., **25**, 4 (2008).
24. J. W. Choi, W. S. Choi, K. H. Lee and B. H. Ha, *J. Korean Institute Chem. Eng*., **32**, 5 (1994).
25. M. A. Rodriguez and J. Ancheyta, *Energy & Fuels*, **18**, 789 (2004).
26. N. Kunisada, K. H. Choi, Y. Korai and I. Mochida, *Appl. Catal. A: Gen.*, **260**, 185 (2004).
27. C. S. Hsu and P. R. Robinson, *Practical advances in petroleum processing*, Volume I, Springer Publication, 1st Ed. (2006).
28. F. S. Mederos, M. A. Rodriguez, J. Ancheyta and E. Arce, *Energy & Fuels*, **20**, 996 (2006).
29. R. J. Angelici, *Polyhedron*, **16**, **18**, 3073 (1997).
30. M. Bhaskar, G. Valavarasu, B. Sairman, K. S. Balaraman and K, Balu, *Ind. Eng. Chem. Res*., **43**, 6654 (2004).
31. G. M. Sanzhez and J. Ancheyta, *Appl. Catal. A: Gen.*, **207**, 407 (2001).
32. R. G. Tailleur, *Comput. Chem. Eng.*, **29**, 2404 (2005).
33. S. Mohanty, D. N. Saraf and D. Kunzru, *Fuel Processing Tech*., **29**, 1 (1991).
34. D. E.Mears, *Chem. Eng. Sci*., **26**, 1361 (1971).
35. G F. Froment and K. B. Bischoff, *Chemical reactor analysis and design*, 2nd Ed., Wiley, New York (1990).
36. M. Baerns, H. Hofmann and A. Renken, *Chemische reaktionstechnik*, George Thieme Verlag, Stuttgart (1987).
37. D. C. Montgomery, *Design and analysis of experiments*, John Wiley & Sons, New York (2001).
38. G M. Clarke and R. E. Kempson, *Introduction to the design and analysis of experiments*, Arnold, London (1997).
39. G. Jing, Y. Jiang and M. H. Al-Dahhan, *Chem. Eng. Sci*., **63**, 751 (2008).
40. O. Levenspiel, *Chem. Reaction Eng*., 3rd Ed., John Wiley & Sons Inc. (2001).
41. V. K. Pareek, Z. Yap, M. P. Brungs and A. A. Adesina, *Chem. Eng. Sci*., **56**, 6063 (2001).
42. S. N. Palaskar, J. K. De and A. B. Pandit, *Chem. Eng. Tech*., **23** (2001).
43. A. Kumar, G M. Ganjyal, D. Jones and M. A. Hanna, *J. Food Eng*., **84**, 441 (2008).
44. P. L. Mills and M. P. Dudukovic, *Ind. Eng. Chem. Fund*., **18**, **2** (1979).
45. T. Ahmed, *Hydrocarbon phase behavior*, Gulf Publishing, Houston (1989).
46. A. Marafi, E. Kam and A. Stanislaus, *Fuel*, **87**, 2131 (2008).
47. M. A. Ali, T. Tatsumi and T. Masuda, *Appl. Catal. A: Gen.*, **233**, 77 (2002).
48. J. Scherzer and A. J. Gruia, *Hydrocracking Sci. and Tech*., CRC Press (1996).
49. J. Singh, M. M. Kumar, A. K. Saxena and S. Kumar, *Chem. Eng. J*., **108**, 239 (2005).